Journal of Biomolecular NMR, **12:** 123–133, 1998.
KLUWER/ESCOM

Conformational analysis of a *Chlamydia*-specific disaccharide α-Kdo-(2→8)-α-Kdo-(2→O)-allyl in aqueous solution and bound to a monoclonal antibody: Observation of intermolecular transfer NOEs

Tobias Sokolowski[a], Thomas Haselhorst[a], Karoline Scheffler[a], Rüdiger Weisemann[b], Paul Kosma[c], Helmut Brade[d], Lore Brade[d] and Thomas Peters[a,*]

[a] *Institut für Chemie, Medizinische Universität Lübeck, Ratzeburger Allee 160, D-23538 Lübeck, Germany* [b] *Bruker Analytik GmbH, Silberstreifen, D-76287 Rheinstetten, Germany* [c] *Institut für Chemie der Universität für Bodenkultur Wien, A-1190 Wien, Austria* [d] *Forschungszentrum Borstel, Zentrum für Medizin und Biowissenschaften Parkallee 22, D-23845 Borstel, Germany*

Received 8 December 1997; Accepted 30 January 1997

Key words: HMQC-trNOESY, Kdo, monoclonal antibody, QUIET-trNOESY, trNOESY, trROESY

Abstract

The disaccharide α-Kdo-(2→8)-α-Kdo (Kdo: 3-deoxy-D-*manno*-oct-2-ulosonic acid) represents a genus-specific epitope of the lipopolysaccharide of the obligate intracellular human pathogen *Chlamydia*. The conformation of the synthetically derived disaccharide α-Kdo-(2→8)-α-Kdo-(2→O)-allyl was studied in aqueous solution, and complexed to a monoclonal antibody S25-2. Various NMR experiments based on the detection of NOEs (or transfer NOEs) and ROEs (or transfer ROEs) were performed. A major problem was the extensive overlap of almost all ^{1}H NMR signals of α-Kdo-(2→8)-α-Kdo-(2→O)-allyl. To overcome this difficulty, HMQC-NOESY and HMQC-trNOESY experiments were employed. Spin diffusion effects were identified using trROESY experiments, QUIET-trNOESY experiments and MINSY experiments. It was found that protein protons contribute to the observed spin diffusion effects. At 800 MHz, intermolecular trNOEs were observed between ligand protons and aromatic protons in the antibody binding site. From NMR experiments and Metropolis Monte Carlo simulations, it was concluded that α-Kdo-(2→8)-α-Kdo-(2→O)-allyl in aqueous solution exists as a complex conformational mixture. Upon binding to the monoclonal antibody S25-2, only a limited range of conformations is available to α-Kdo-(2→8)-α-Kdo-(2→O)-allyl. These possible bound conformations were derived from a distance geometry analysis using transfer NOEs as experimental constraints. It is clear that a conformation is selected which lies within a part of the conformational space that is highly populated in solution. This conformational space also includes the conformation found in the crystal structure. Our results provide a basis for modeling studies of the antibody–disaccharide complex.

Introduction

The saccharide 3-deoxy-D-*manno*-oct-2-ulosonic acid (Kdo) is an essential part of the lipopolysaccharide (LPS) of gram-negative bacteria. The sequence α-Kdo-(2→8)-α-Kdo is found exclusively in LPS of the genus *Chlamydia* (Brade et al., 1997). These pathogenic, obligatory intracellular parasites are responsible for a variety of diseases in animals and humans. During infection, antibodies are expressed against components in the outer membrane, whereby LPS is one of the major surface antigens. Therefore, it plays an important role during infection. Several monoclonal antibodies were raised against distinct epitopes of the carbohydrate moiety of chlamydial LPS (Fu et al., 1992). The monoclonal antibody S25-2 binds to the trisaccharide α-Kdo-(2→8)-α-Kdo-(2→4)-α-Kdo and to the disaccharide α-Kdo-(2→8)-α-Kdo with high affinity. Binding was also observed with the (2→4)-linked dis-

*To whom correspondence should be addressed.

accharide, however, with lower affinity. LPS-specific antibodies are potential tools for the diagnosis and therapy of *Chlamydia* infections and, therefore, an understanding of the molecular basis of their interaction with antigenic carbohydrates is desirable. Under certain conditions, these interactions can be studied with transfer NOE (trNOE) experiments (Ni, 1994).

Although a variety of saccharides have already been studied utilizing trNOE experiments (Peters and Pinto, 1996), the disaccharide α-Kdo-(2→8)-α-Kdo-(2→O)-allyl (Kosma et al., 1990) is of specific interest since it contains a very flexible glycosidic linkage leading to an almost complete overlap of all ^{1}H NMR signals. For this reason, in a previous NMR investigation of this disaccharide and related derivatives, no attempt was made to perform an in-depth conformational analysis of α-Kdo-(2→8)-α-Kdo-(2→O)-allyl (Bock et al., 1992). In the following, the detailed conformational analysis of the conformation of this disaccharide in aqueous solution, and bound to the monoclonal antibody S25-2, will be described.

Materials and Methods

Preparation of the NMR sample

NMR experiments with the uncomplexed disaccharide were performed using a sample of 1.5 mg (2.7 μmol) of α-Kdo-(2→8)-α-Kdo-(2→O)-allyl (disodium salt, monohydrate) dissolved in 500 μl D_2O (99.998%). The disaccharide was freeze dried and dissolved in D_2O four times prior to sample preparation.

The complex was prepared with 5 mg (33.3 nmol) monoclonal antibody S25-2 (IgG-type) and 540 μg (0.96 μmol) of α-Kdo-(2→8)-α-Kdo-(2→O)-allyl (disodium salt, monohydrate) in 554 μl PBS (15 mm phosphate, 10 mm NaCl, pH 6.8) leading to a concentration of 60.1 μM for the antibody and 1.7 mM for the disaccharide. This corresponds to a molar ratio of 1:14 of antibody binding sites to carbohydrate. The solvent was D_2O (99.998%). Prior to sample preparation, H_2O was exchanged against D_2O by repeated cycles of freeze drying and dissolving.

NMR experiments

NMR experiments with the uncomplexed disaccharide were carried out on a Bruker Avance 500 spectrometer (Institut für Chemie, Medizinische Universität Lübeck). Experiments with the complex were performed on Bruker Avance 500, Avance 600 (Institut für Biophysikalische Chemie, Johann Wolfgang Goethe Universität Frankfurt) and Avance 800 (Bruker Analytik GmbH) spectrometers. All spectra were recorded at 310 K without sample spinning. Data acquisition and processing were performed with XWINNMR software (Bruker) running on Silicon Graphics Indy II workstations. For integration of NOE signals, the programs AURELIA (Bruker) or XWINNMR were used.

2D NOESY experiments with the uncomplexed disaccharide were performed at 500.13 MHz, and 512 (t_1) ×2K (t_2) data points were recorded. Prior to Fourier transformation the data matrix was zero filled to 2K × 4K and multiplied with squared cosine functions. The spectral width was 8 ppm in F1 and F2. For the relaxation delay 3.5 s was used. The mixing time was 800 ms. HDO signal suppression was achieved by low-power irradiation for 1 s during the relaxation time and during the mixing time. A total of 32 scans per increment and 16 dummy scans were performed.

The 2D trNOESY experiments were performed at 600.13 and 800.13 MHz. A 2D NOESY sequence with a spin-lock filter (Scherf and Anglister, 1993) to suppress protein resonances was used. The spectral width was set to 6 or 10 ppm; 512 increments were recorded in t_1 and 2K data points in t_2. After 64 dummy scans, 64 scans were performed per increment. The HDO signal was suppressed by presaturation with low-power irradiation during the relaxation and mixing time. A spin-lock field of 5 kHz with a length of 10 ms after the first 90° pulse was used to suppress protein signals. A relaxation time of 1.2 s and mixing times of 25–400 ms were used. Prior to Fourier transformation, zero filling in t_1 and multiplication with squared cosine functions in each dimension were applied to yield matrices of 1K × 2K data points.

Standard 2D HMQC-NOESY and HMQC-trNOESY experiments were performed at 500.13 MHz for ^{1}H and 125.77 MHz for ^{13}C, respectively. A data matrix of 256 × 2K points was recorded, zero filled to 512 × 2K and multiplied by squared cosine functions prior to Fourier transformation. The spectral width was 10 ppm in F2 and 120 ppm in F1. Low-power irradiation during relaxation and mixing time was applied to suppress the HDO signal. The HMQC-NOESY experiment was performed using a mixing time of 900 ms and a relaxation time of 1.2 s; 128 dummy scans and 704 scans per increment were performed. For the HMQC-trNOESY experiment, a relaxation time of 400 ms and a mixing time of 300 ms were used; 128 dummy scans at the beginning of the experiment and 2K scans per increment were performed.

The total experimental time for both experiments was about 4.5 days.

The 2D ROESY experiment was performed at 500.13 MHz. A T-ROESY pulse sequence was used (Hwang and Shaka, 1992), and 512 × 2K data points were recorded. Prior to Fourier transformation, the data set was zero filled to 1K × 2K and multiplied with squared cosine functions. A spectral width of 10 ppm in both dimensions, 16 dummy scans and 32 scans per increment were used. The HDO signal was suppressed by low-power irradiation for 1 s during the relaxation time. The total relaxation time was 3.7 s. The ROESY spin-lock field had a strength of 1.1 kHz and a length of 800 ms.

For the trROESY experiment, 600 × 8K data points were recorded, zero filled to give a matrix of 2K × 8K and multiplied with squared cosine functions prior to Fourier transformation. The spectral width was 10 ppm in F1 and F2. After 96 dummy scans, 48 scans per increment were performed. The relaxation time was 2 s. The HDO signal was suppressed by low-power irradiation for 1.5 s during the relaxation time. A 250 ms ROESY spin lock of 2.7 kHz was used.

2D QUIET-NOESY experiments (Vincent et al., 1997) were performed at 500.13 MHz. A modified NOESY sequence was used. After the first 90° pulse, the protein signals were suppressed by a spin-lock field (5 kHz, 10 ms). In the middle of the mixing time (250 ms), a Gaussian pulse or a Q3 cascade (Emsley and Bodenhausen, 1992) was used for the double selective inversion. A homospoil gradient (1 ms, 5 G/cm) at the end of the mixing time was implemented in order to improve the spectra quality. A total of 512 × 2K data points were recorded, zero filled to 1K × 2K, and multiplied with squared cosine functions prior to Fourier transformation. The spectral width was 10 ppm in F1 and F2. HDO signal suppression was achieved by low power irradiation for 1s during the relaxation time.

1D transient NOE experiments with saturation of one spin during the mixing time (MINSY experiments) (Massefski and Redfield, 1988) were recorded at 500.13 MHz. The spectral width was set to 10 ppm; 16K data points were acquired and, prior to Fourier transformation, the FIDs were multiplied by exponential functions. A 180° Gaussian pulse of 200 ms duration was employed for selective inversion of $H4^b$. In order to prevent an inversion of the proton $H5^b$ that resonates only 0.05 ppm apart, $H5^b$ was presaturated by low-power irradiation for 1 s during the relaxation delay. The total relaxation delay was 2.6 s. During the mixing time of 250 ms the protons $H5^b$ or $H6^b$ were saturated by irradiation at their respective chemical shifts.

Metropolis Monte Carlo simulations

Metropolis Monte Carlo (MMC) simulations were performed on Silicon Graphics O2 R10000 workstations with the program GEGOP (Stuike-Prill and Meyer, 1991; Peters et al., 1993). A set of conformations was generated by 2×10^6 macrosteps and a temperature parameter of 1000 K. The following definitions of torsion angles were used: $\Phi^a = C1^a\text{-}C2^a\text{-}O8^a\text{-}C8^b$, $\Psi^a = C2^a\text{-}O8^b\text{-}C8^b\text{-}C7^b$, $\omega_1^a = H7^a\text{-}C7^a\text{-}C6^a\text{-}H6^a$, $\omega_2^a = O8^a\text{-}C8^a\text{-}C7^a\text{-}O7^a$, $\Phi^b = C1^b\text{-}C2^b\text{-}O1^{allyl}\text{-}C1^{allyl}$, $\Psi^b = C2^b\text{-}O1^{allyl}\text{-}C1^{allyl}\text{-}C2^{allyl}$, $\omega_1^b = H7^b\text{-}C7^b\text{-}C6^b\text{-}H6^b$, $\omega_2^b = O8^b\text{-}C8^b\text{-}C7^b\text{-}O7^b$, $\chi = O1^{allyl}\text{-}C1^{allyl}\text{-}C2^{allyl}\text{-}C3^{allyl}$. The maximum step size for torsion angles was 20°. This leads to a total acceptance rate of 55%. NOE relaxation matrices based upon $<r^{-6}>$ values were summed to yield a full relaxation matrix. With the full relaxation matrix, theoretical ensemble-averaged NOEs were calculated (Weimar et al., 1997) for a mixing time of 800 ms. Different overall correlation times were fitted to a reasonable agreement with experimental values. The best results were obtained with a correlation time of 150 ps. Similarly, NOEs expected for the crystal structure were calculated. The full relaxation matrix was also calculated with GEGOP using the coordinates of the X-ray structure. Mixing and correlation times were set as above.

The conformational space of the disaccharide in the bound state was determined with distance constraints obtained from trNOE experiments. A distance constraint of 2–4 Å was set for two protons that exhibited a trNOE. The following trNOEs were used as distance constraints: $H4^a/H2^{allyl}$, $H6^b/H2^{allyl}$, $H4^a/H3_Z^{allyl}$, $H4^b/H3_Z^{allyl}$, $H6^b/H3_Z^{allyl}$. Moreover, the trNOEs $H6^a/H8^b$ and $H6^a/H1^{allyl}$ were observed but could not be assigned stereospecifically. Therefore, in calculations the combinations of $H6^a/H8^b_{proR}$ or $H6^a/H8^b_{proS}$ and $H6^a/H1^{allyl}_{proR}$ or $H6^a/H1^{allyl}_{proS}$ were used. This leads to four different sets, each comprising seven distance constraints. The MMC simulation with 2×10^6 macrosteps yielded 1.1×10^6 accepted conformations. About 1000 conformations out of these 1.1×10^6 conformations matched the constraints. Only minor differences were found by using the four different constraint sets.

Results and Discussion

This study is divided into two major parts: one covering the conformational analysis of the disaccharide α-Kdo-(2→8)-α-Kdo-(2→O)-allyl in aqueous solution and the other describing the analysis of the conformation of α-Kdo-(2→8)-α-Kdo-(2→O)-allyl bound to the monoclonal antibody S25-2. The conformational analysis of the free disaccharide employed NMR experiments and MMC simulations. The bound conformation of α-Kdo-(2→8)-α-Kdo-(2→O)-allyl was deduced from trNOESY, QUIET-trNOESY and tr-ROESY experiments. Chemical shifts and coupling constants were in accordance with the values reported before and are summarized in Tables 1 and 2.

Table 1. ^{1}H and ^{13}C chemical shifts of α-Kdo-(2→8)-α-Kdo-(2→O)-allyl

	Unit a α-Kdo-(2→ (ppm)	Unit b -α-Kdo- -(2→ (ppm)	Allyl →O)-allyl (ppm)
$H3_{ax}$	1.79	1.79	
$H3_{eq}$	2.03	2.05	
H4	4.03	4.09	
H5	3.97	4.03	
H6	3.57	3.66	
H7	3.92	3.98	
H8′	3.63	3.62	
H8″	3.89	3.62	
$H1'^{allyl}$			3.96
$H1''^{allyl}$			3.86
$H2^{allyl}$			5.96
$H3_{E}^{allyl}$			5.24
$H3_{Z}^{allyl}$			5.34
C3	34.7	34.7	
C4	66.6	66.7	
C5	66.8	67.0	
C6	72.5	72.0	
C7	70.0	68.4	
C8	63.7	65.4	
$C1^{allyl}$			64.8
$C2^{allyl}$			134.7
$C3^{allyl}$			118.0

Chemical shifts were measured in D_2O at 310 K. The spectrometer frequency was 500.13 MHz for ^{1}H or 125.77 MHz for ^{13}C. Trimethylsilyl propionic acid was used as the reference. Chemical shifts are in accordance with previously reported values (Bock et al., 1992).

Conformational analysis of α-Kdo-(2→8)-α-Kdo-(2→O)-allyl

As noticed before, the ^{1}H NMR spectrum of α-Kdo-(2→8)-α-Kdo-(2→O)-allyl displays severe overlap of nearly all resonance signals. This is obvious from Figure 2, which demonstrates that only two resonance signals, $H6^{a}$ and $H4^{b}$, are slightly separated. Therefore, a conformational analysis based on NMR experiments is difficult. Vicinal $^{1}H,^{1}H$ coupling constants for the pyranose rings (Table 1) show that both rings occupy the $^{5}C_2$ conformation. For the analysis of the glycosidic linkage orientation, the vicinal coupling constants $^{3}J(H6^{b}, H7^{b})$, $^{3}J(H7^{b}, H8^{b}_{proR})$ and $^{3}J(H7^{b}, H8^{b}_{proS})$ are important. $^{3}J(H6^{b}, H7^{b})$ is 9.0 Hz and indicates a trans orientation of the respective protons. Unfortunately, the protons $H8^{b}_{proS}$ and $H8^{b}_{proR}$ resonate at nearly the same frequency, and therefore cannot be used to analyze the orientation of the C7-C8 bond. The resonance signal of $H7^{b}$ overlaps only with the one of $H5^{a}$, and, after performing an adequate apodization with a Gaussian window function, allows a first-order analysis of the coupling constants $^{3}J(H7^{b}, H8^{b}_{proR})$ and $^{3}J(H7^{b}, H8^{b}_{proS})$. A stereospecific assignment of the protons $H8^{b}_{proR}$ and $H8^{b}_{proS}$ is still impossible, but values of 3.5 and 4.5 Hz (Table 2) are in accordance with the gauche orientation around the $C7^{b}$-$C8^{b}$ bond as found in the crystal structure of α-Kdo-(2→8)-α-Kdo-(2→O)-allyl. Therefore, we assume that the conformations around the glycosidic bond torsion angles ω_1^{b} and ω_2^{b} (for a definition see Figure 1) are similar to the ones in the crystal structure. The orientation of the $C6^{a}$-$C7^{a}$-$C8^{a}$ side chain can be deduced from the corresponding vicinal coupling constants (Table 2), as this has been described before. A trans orientation is preponderant around the $C6^{a}$-$C7^{a}$ bond whereas a rotamer equilibrium is found around the $C7^{a}$-$C8^{a}$ bond.

In a previous study, no interglycosidic NOEs were described. An inspection of 2D NOESY spectra clearly shows the presence of a strong interglycosidic NOE between $H6^{a}$ and $H8^{b}$ (Figure 3). A distinction between $H8^{b}_{proR}$ and $H8^{b}_{proS}$ is not possible. In the crystal structure of α-Kdo-(2→8)-α-Kdo-(2→O)-allyl, a short distance between $H8^{b}_{proR}$ and $H6^{a}$ of 2.7 Å corresponds well with the observed interglycosidic NOE (Figure 3). To improve the signal dispersion, a 2D HMQC-NOESY spectrum was acquired. No further interglycosidic NOEs were observed in this spectrum but two intraglycosidic NOEs between $H6^{b}$ and $H8^{b}$ and between $H5^{b}$ and $H7^{b}$ are observed. These NOEs are sensitive to the size of the torsion angles ω_1^{b} and ω_2^{b}. Both NOEs are in accordance

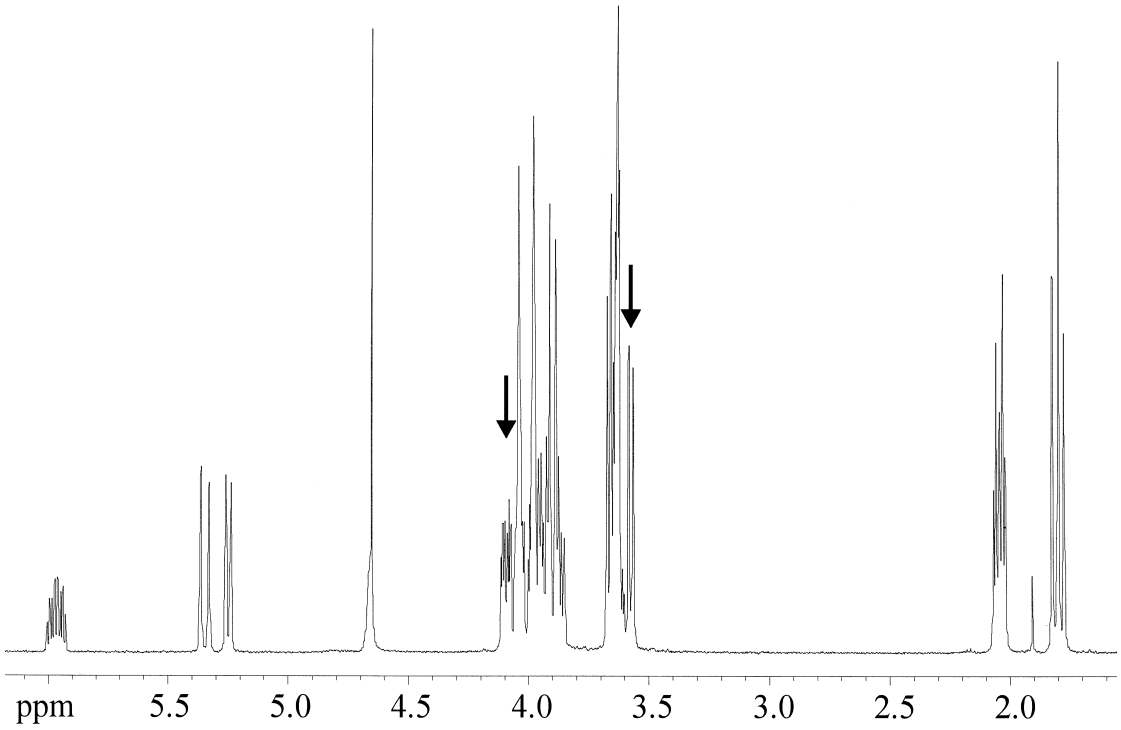

Figure 1. ^{1}H-NMR spectrum of α-Kdo-(2→8)-α-Kdo-(2→O)-allyl. All carbohydrate resonances overlap except for the signals of H4^b (4.09 ppm) and H6^a (3.57 ppm) that are labeled with arrows.

Table 2. First-order $J_{H,H}$ coupling constants

	Unit a α-Kdo-(2→ (Hz)	Unit b -α-Kdo-(2→ (Hz)
$H3_{ax}/H3_{eq}$	−13.0	−13.0
$H3_{ax}/H4$	12.0	12.0
$H3_{eq}/H4$	5.0	5.0
H4/H5	3.0	3.0
H5/H6	1.0	1.0
H6/H7	9.0	9.0
H7/H8′	6.5	4.5
H7/H8″	2.5	3.5
H8’/H8″	−12.0	−10.0

Coupling constants were reported previously (Bock et al., 1992).

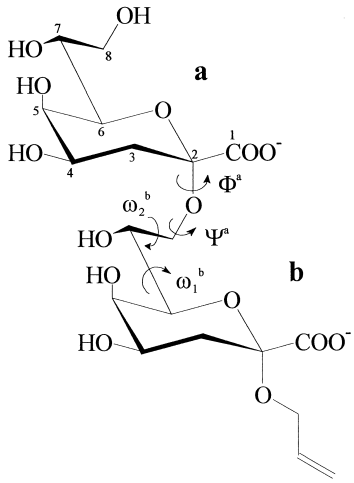

Figure 2. Formula of α-Kdo-(2→8)-α-Kdo-(2→O)-allyl. The following definitions of glycosidic angles were used: Φ^a = C1^a-C2^a-O8^b-C8^b, Ψ^a = C2^a-O8^b-C8^b-C7^b, Φ^b = C1^b-C2^b-O1^{allyl}-C1^{allyl}, Ψ^b = C2^b-O1^{allyl}-C1^{allyl}-C2^{allyl}, ω_1 = H7-C7-C6-H6, ω_2 = O8-C8-C7-O7.

with the crystal structure of α-Kdo-(2→8)-α-Kdo-(2→O)-allyl (Mikol et al., 1994) (H5^b-H7^b = 3.26 Å, H6^b-H8$^b_{proR}$ = 3.16 Å, H6^b-H8$^b_{proS}$ = 3.75 Å), and thus substantiate our hypothesis that the orientations around the C6^b-C7^b and the C7^b-C8^b bonds in solution are similar to the conformations found in the crystalline state.

The side chain of the non-reducing Kdo unit a, on the other hand, shows different orientations in solution and in the crystal structure. As mentioned above,

a coupling constant $^3J(H7^a, H6^a)$ of 9 Hz indicates a preponderant trans orientation around the $C6^a$-$C7^a$ bond (ω_1^a angle), whereas in the crystalline state $H7^a$ and $H6^a$ are gauche oriented, probably due to packing effects.

The orientation of the allyl group in the crystalline state predicts NOEs that are only partly observed indicating different conformations of the allyl group in solution and in the crystal. Most important, a short distance is found between $H1^{allyl}_{proR}$ and $H4^a$ in the crystal structure (2.8 Å). No corresponding interglycosidic NOE is observed (Table 3). In general, only weak NOEs are detected between pyranose ring protons and protons of the allyl group. Some interglycosidic NOEs exclude each other and, therefore, several conformations are possible for the allyl group in aqueous solution. Experimental NOEs and NOEs predicted from the crystal structure are compared in Table 3.

It is concluded that the crystal structure gives a reasonable model for the predominant relative orientation of the two pyranose rings in aqueous solution. The conformation of the side chain of the non-reducing unit a and the conformation of the O-allyl group cannot reliably be predicted by the crystal structure. Because of the lack of a sufficient amount of interglycosidic NOE data, no attempt was made to perform a quantitative comparison between a theoretical conformational model and experimental NOE data. Nevertheless, MMC simulations were performed to allow a qualitative comparison. These data are also included in Table 3. A brief summary of the MMC simulations is given in the following.

MMC simulations of 2×10^6 macrosteps were performed with the temperature parameter set at 1000 K. A high-temperature parameter is necessary to ensure that the whole sterically accessible conformational space will be explored (Scheffler et al., 1995). Scatter plots are shown in Figure 5. It is seen that the major population of conformers is characterized by a dihedral angle Φ^a of $-60°$ at the glycosidic linkage as found in the crystal structure. Two minima are observed for the glycosidic angle Ψ^a, namely at 130° and 210°. In the crystal structure a value of 132° is found. The torsional angles of the side chain of unit b, ω_1^b and ω_2^b, in the glycosidic linkage display high flexibility. For Φ^b and Ψ^b, the glycosidic torsion angles in the linkage between unit b and the allyl group, similar minima are found as for Φ^a and Ψ^a (Figure 4). With a full relaxation matrix, obtained by the MMC simulations, theoretical NOEs were calculated (Table 3). Also, NOEs predicted from the crystalline structure of α-Kdo-(2→8)-α-Kdo-(2→O)-allyl are included in Table 3. Most of the experimentally observed NOEs are predicted by the MMC simulation.

Conformational analysis of α-Kdo-(2→8)-α-Kdo-(2→O)-allyl bound to S25-2

In comparison with the NOESY spectrum of uncomplexed α-Kdo-(2→8)-α-Kdo-(2→O)-allyl, the trNOESY spectrum of the disaccharide in complex with the monoclonal antibody S25-2 shows a different cross peak pattern. In the trNOESY experiment, some additional cross peaks are observed (Figure 3). It is important to note that this might not indicate that the bound conformation is different from the conformational family that predominates in solution. First, it is necessary to prove that additional cross peaks can be explained by trNOEs. It is well known that spin diffusion may lead to a misinterpretation of trNOESY experiments (Arepalli et al., 1995). For this reason, trROESY experiments have to be performed. Another experiment that has been suggested lately for the elimination of spin diffusion effects is the QUIET-NOESY experiment (Zwahlen et al., 1994; Vincent et al., 1997). It is shown in the following that the trROESY and QUIET-trNOESY experiments are essential for a detailed analysis of the α-Kdo-(2→8)-α-Kdo-(2→O)-allyl/S25-2 complex.

One interglycosidic trNOE between $H6^a$ and $H8^b$ is observed. It matches the corresponding NOE in the free disaccharide. The HMQC-trNOESY spectrum shows the trNOEs $H6^b/H8^b$ and $H5^b/H7^b$, although the latter is rather weak compared to the corresponding NOE in the free disaccharide. In addition to these trNOEs, which match NOEs for the free disaccharide, some cross peaks occur that are absent in aqueous solution, for example $H4^b/H8^b$ and $H4^a$,$H5^b/H8^b$ (Figure 3). The resonance signals of $H4^a$ and $H5^b$ overlap. Even high-field trNOESY experiments at 800 MHz do not resolve the signals. Since the resonance frequencies of $C4^a$ and $C5^b$ are also almost identical (Table 1), HMQC-trNOESY spectra cannot resolve the trNOEs $H4^a/H8^b$ and $H5^b/H8^b$ either. Another difference between free and bound forms of the disaccharide is observed for the cross-peak pattern involving the allyl protons. The cross peaks $H3^{allyl}_E/H4^a$ and $H3^{allyl}_E/H6^b$ observed for the free disaccharide are not detected in trNOESY spectra.

To identify spin diffusion pathways, trROESY experiments were performed (Arepalli et al., 1995; Weimar et al., 1995). In general, trROEs for the dis-

Table 3. Relative NOEs[a] from NMR experiments, crystal structure and MMC calculations

NOE	Experiment aqueous solution[b]	MMC simulation[c]	Crystal structure[d]	Experiment complex[e]
$H6^a/H8^b_{proR}$		44	27	
	} 40[f]			} 22[f]
$H6^a/H8^b_{proS}$		−2[g]	3	
$H6^b/H8^b_{proR}$		19	15	
	} n.d.[h]			} n.d.[h]
$H6^b/H8^b_{proS}$		22	3	
$H1^{allyl}_{proR}/H4^a$	–	6	13	–
$H1^{allyl}_{proR}/H6^a$	–	4	22	–
$H1^{allyl}_{proR}/H6^b$	n.d.[h]	73	44	n.d.[h]
$H1^{allyl}_{proR}/H8^b_{proR}$	–	4	19	–
$H1^{allyl}_{proS}/H6^a$	13	1	−1[g]	–
$H1^{allyl}_{proS}/H6^b$	–	2	−3[g]	–
$H2^{allyl}/H3^a_{eq}$	–	1	17	–
$H2^{allyl}/H4^a$		5	200	
	} 13[f]			} 15[f]
$H2^{allyl}/H5^b$		–	–	
$H2^{allyl}/H6^b$	17	29	26	20
$H3^{allyl}_Z/H4^a$		2	18	
	} 6[f]			} 8[f]
$H3^{allyl}_Z/H5^b$		–	–	
$H3^{allyl}_Z/H4^b$	5	–	–	5
$H3^{allyl}_Z/H6^b$	11	−1[g]	–	8
$H3^{allyl}_E/H4^a$		2	4	–
	} 7[f]			
$H3^{allyl}_E/H5^b$		–	–	–
$H3^{allyl}_E/H6^b$	3	13	1	–
$H3^{allyl}_E/H8^b_{proR}$	–	1	–	–
$H3^{allyl}_E/H8^b_{proS}$	–	1	–	–

[a] All values in% of the intraglycosidic NOE $H4^b/H6^b$.
[b] Mixing time 800 ms, experimental temperature 310 K.
[c] Mixing time 800 ms, simulation at 1000 K (see experimental section).
[d] Mixing time 800 ms.
[e] trNOEs, mixing time 250 ms, experimental temperature 310 K.
[f] Experimental discrimination between $H4^a$ and $H5^b$ is impossible.
[g] Negative values resulting from indirect contacts.
[h] NOE is present but intensity cannot be determined due to signal overlap.

accharide α-Kdo-(2→8)-α-Kdo-(2→O)-allyl are positive and cross peaks resulting from spin diffusion via one relay spin would be negative, allowing an easy discrimination between direct and indirect (spin diffusion) magnetization transfer. A complication arises if indirect and direct effects overlap because the respective positive and negative signals may add to zero. In this case, trROEs might be misinterpreted as spin diffusion although a direct dipolar interaction exists. trROESY spectra of α-Kdo-(2→8)-α-Kdo-(2→O)-allyl complexed with S25-2 show only signals that are also observable for the disaccharide in aqueous solution. This indicates that the bound conformation of α-Kdo-(2→8)-α-Kdo-(2→O)-allyl is similar to conforma-

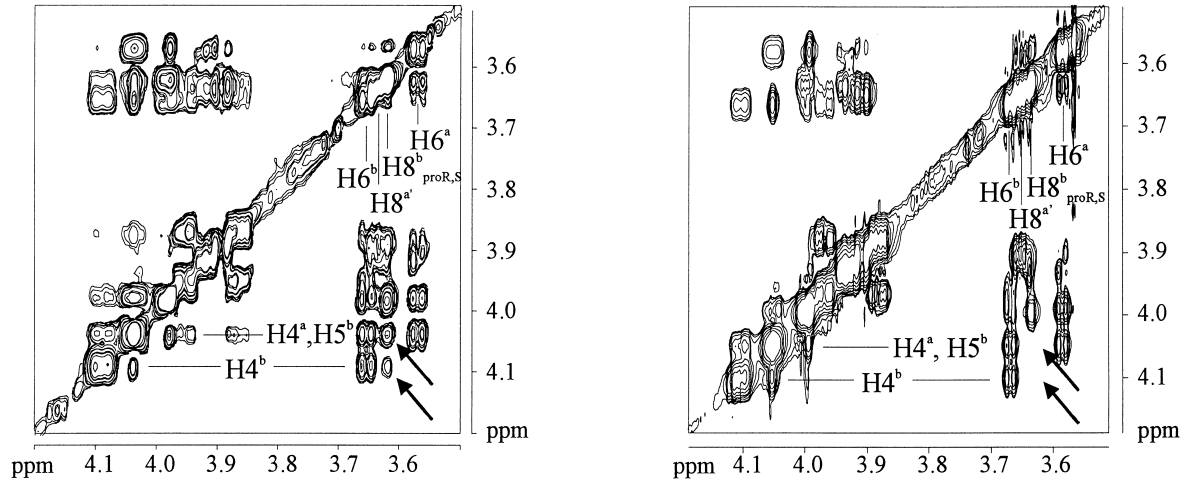

Figure 3. Left: Expansion of the 600 MHz trNOESY spectrum of α-Kdo-(2→8)-α-Kdo-(2→O)-allyl. Cross peaks arising from spin diffusion ($H4^b/H8^b$ and $H4^a,H5^b/H8^b$) are marked with arrows. Right: Expansion of the 800 MHz trROESY spectrum of α-Kdo-(2→8)-α-Kdo-(2→O)-allyl. The disappearance of spin diffusion peaks is marked with arrows.

tions that predominate in aqueous solution. To verify that spin diffusion contributes to cross peaks only observed in trNOESY experiments but not in trROESY experiments, so-called QUIET-trNOESY experiments were performed (Vincent et al., 1997). These experiments apply a double or multiple selective pulse during the mixing time inverting spins that are suspicious to be involved in spin diffusion. A QUIET-trNOESY experiment with inversion of all protons between 3.5 and 4.2 ppm displays the same cross-peak pattern as the trNOESY spectrum. If aliphatic or aromatic protons of the protein mediate spin diffusion, a different pattern would be expected. In contrast, all signals determined as spin diffusion by trROESY experiments are present in this QUIET-trNOESY spectrum. In a second QUIET-trNOESY experiment a double selective pulse was applied that inverts $H4^b$, $H4^a$, $H5^b$ and $H6^b$, $H8^{a'}$, $H8^b$. The resulting spectrum shows that the cross peaks $H4^b/H8^b$ and $H4^a,H5^b/H8^b$ are present. This indicates that direct interactions are present in addition to spin diffusion effects, leading to zero intensity in the trROESY spectrum as discussed above. In order to identify the relay spins that are responsible for spin diffusion, additional experiments have to be performed and cross-peak intensities from trNOESY and QUIET-trNOESY spectra can be compared. Spin diffusion via protein protons is most elegantly demonstrated by the detection of trNOEs between protein and ligand protons. Unfortunately, the intensities of intermolecular trNOEs are very weak (Moseley et al., 1997) and difficult to detect. To overcome the sensitivity problem, we performed trNOESY experiments at 800 MHz in which contacts between ligand and protein are observed (Figure 5). Intermolecular trNOEs are detected between aromatic protons of the antibody and the ligand protons $H4^a$, $H5^b$ and $H7^b$, $H5^a$. Because $H4^a$ and $H5^b$ have almost identical chemical shifts, and the same holds for $H7^b$ and $H5^a$(Table 1), it is impossible to discriminate between these protons at this stage, but it is unambiguous that aromatic side-chain protons of the protein are involved in spin diffusion effects as discussed above.

One remaining problem is the trNOE between $H4^b$ and $H8^b$. The QUIET-trNOESY experiment indicates a direct contact between these two protons, which is not compatible with sterically allowed conformations of the disaccharide. Since the QUIET-trNOESY experiments could only exclude spin diffusion via protein protons but could not give any information about spin diffusion within the ligand, due to the limited selectivity of the shaped pulses, subsequent experiments were necessary. Therefore, we performed a 1D MINSY experiment (Massefski and Redfield, 1988). After selective inversion of $H4^b$, $H6^b$ was saturated during the mixing time, leading to a 1D transient NOE spectrum in which the intensity of the NOE $H4^b/H8^b$ was significantly reduced compared to the 1D transient NOE spectrum without saturation of $H6^b$. This indicates that spin diffusion within the ligand via the pathway $H4^b \rightarrow H6^b \rightarrow H8^b$ plays a role. In the QUIET-trNOESY experiment, $H8^b$ and $H6^b$ could not be inverted separately because the required pulse lengths were too

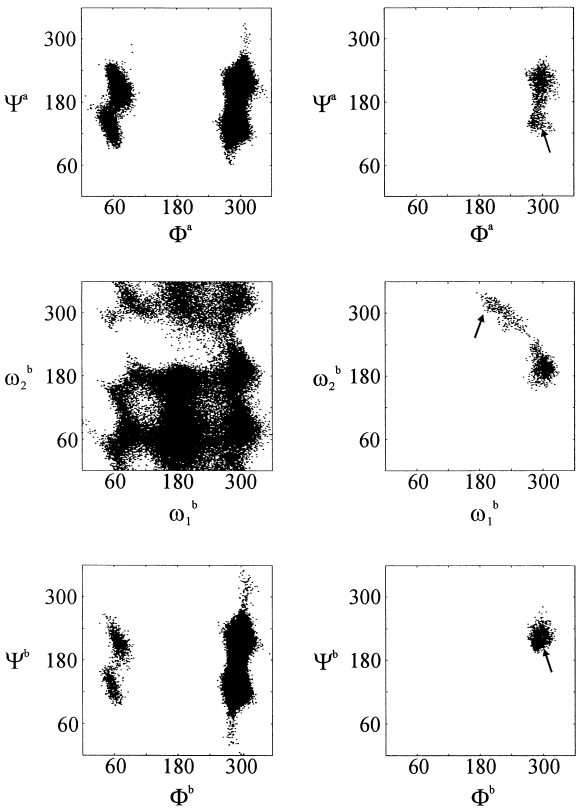

Figure 4. Scatter plots for a 1000 K MMC simulation of α-Kdo-(2→8)-α-Kdo-(2→O)-allyl. Each dot represents a conformation that has been visited during the simulation as a function of the respective angles. Left: Accepted conformations of the MMC simulation at 1000 K. Right: Only conformations within the distance constraints extracted from trNOESY experiments are shown. The choice of constraints is discussed in the text. The conformation found in the crystal structure is marked by arrows.

long, introducing relaxation artifacts. Therefore, the cross peak $H4^b/H8^b$ in the trNOESY and QUIET-trNOESY spectra most likely results from pure spin diffusion involving also ligand protons.

To separate direct magnetization transfer from spin diffusion, the intensities of the trNOESY and QUIET-trNOESY cross peaks may be compared. Therefore, QUIET-trNOESY signals were integrated and the volumes were compared to the volumes of the corresponding trNOESY signals. Table 4 shows the change of intensities for selected cross peaks. In general, cross peaks from QUIET-trNOESY spectra are about 3–10% smaller than from a corresponding trNOESY experiment. This loss of intensities can be explained by leakage to protein protons. Interestingly, cross peaks belonging to $H5^b$, for example $H5^b/H6^b$ and $H5^b$,$H4^a/H8^b$, are more reduced than others, indicating that $H5^b$ is more significantly affected by spin diffusion. This observation corresponds well with the observed intermolecular trNOEs described above.

Table 4. Intensity changes of trNOEs in trNOESY versus QUIET-trNOESY experiments

trNOE	Rel. intensity in trNOESY (%) experiment	Rel. intensity in QUIET-trNOESY (%) experiment	Rel. intensity change (%)
$H6^a/H5^a$	−13.8	−13.4	2.9
$H6^a/H4^a$	−11.0	−10.7	2.7
$H6^b/H5^b$	−13.6	−12.5	8.1
$H6^b/H4^a$	−10.4	−9.9	4.8
$H5^b$,$H4^a/H8^b$	−8.9	−8.0	10.1

Experimental parameters for QUIET-trNOESY and trNOESY experiments were set at identical values (e.g. mixing time = 250 ms, T = 300 K). All intensities are relative to the diagonal signal of $H4^b$ (−100%) in the respective spectrum.

The experimental trNOEs were used to perform distance constraint calculations on the basis of the high-temperature MMC simulation discussed above. trNOEs were translated into distance constraints (Scheffler et al., 1995) as described under the Materials and Methods section. The allowed conformational states are shown in Figure 4. A further analysis (data not shown) shows that not all combinations of ω_1^b, ω_2^b and ϕ^a, ι^a are allowed. ω_1^b/ω_2^b angles at 220°/−60° correspond to ϕ^a/ι^a angles of −60°/150°. It is obvious that the crystal structure is within the range of possible bound conformations (Figure 4).

Conclusion

The data presented clearly show that a monoclonal antibody that specifically recognizes the disaccharide α-Kdo-(2→8)-α-Kdo linkage binds a conformation of the synthetic disaccharide α-Kdo-(2→8)-α-Kdo-(2→O)-allyl that is also present in aqueous solution. Moreover, a comparison with the crystal structure of α-Kdo-(2→8)-α-Kdo-(2→O)-allyl (Figure 6) (Mikol et al., 1994) indicates that this conformation lies well within the range of possible bound conformations. trNOESY spectra acquired at 800 MHz allowed the detection of intermolecular trNOEs that involve aromatic side-chain protons of the antibody. Four ligand protons ($H4^a$, $H5^a$, $H5^b$ and $H7^b$) were identified to be possibly involved in this contact.

Our results provide an experimental basis to perform docking studies using the crystal structure of F_{ab}

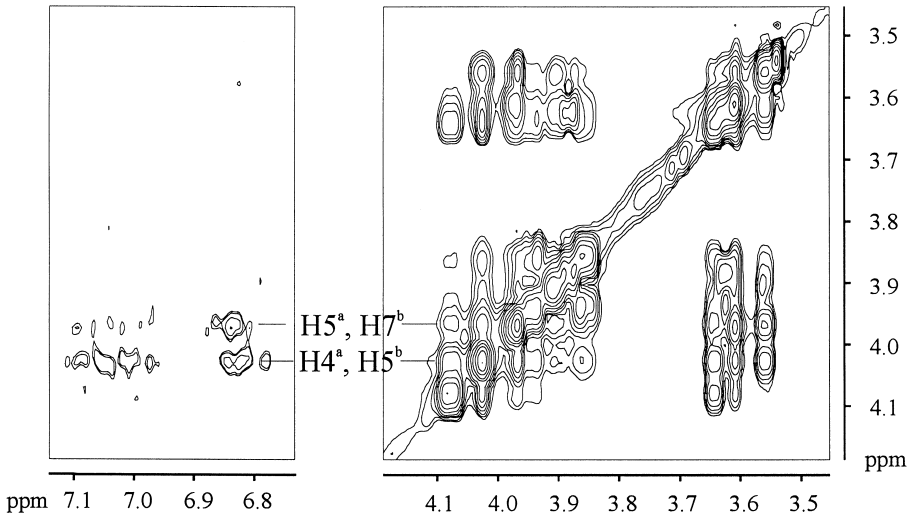

Figure 5. Contacts between protein and carbohydrate protons. Expansions of the 800 MHz trNOESY spectrum of α-Kdo-(2→8)-α-Kdo-(2→O)-allyl. Contacts of $H5^a$, $H7^b$ and $H4^a$, $H5^b$ with aromatic protons of the protein are observed.

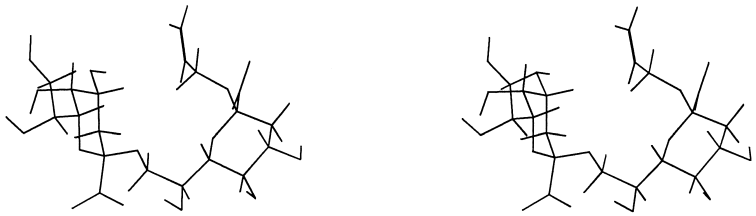

Figure 6. Stereo plot of the crystal structure of α-Kdo-(2→8)-α-Kdo-(2→O)-allyl (disodium salt, monohydrate) (Mikol et al., 1994). Sodium atoms and water molecules are not shown.

fragments of the monoclonal antibody S25-2 that has been solved recently (S. Evans et al., in preparation).

Acknowledgements

This work was supported by a grant of the Deutsche Forschungsgemeinschaft (SFB 470, Teilprojekte B3 and C1) and by the Fonds der Chemischen Industrie. We are indebted to Prof. Dr. H. Rüterjans (Institut für Biophysikalische Chemie, Universität Frankfurt) for giving us access to the 600 MHz spectrometer.

References

Arepalli, S.R., Glaudemans, C.P.J., Daves, G.D., Kovac, P. and Bax, A. (1995) *J. Magn. Reson.*, **B106**, 195–198.

Asensio, J.L., Cañada, F.J. and Jimenez-Barbero, J. (1995) *Eur. J. Biochem.*, **233**, 618–630.

Bock, K., Thomsen, J.U., Kosma, P., Christian, R., Holst, O. and Brade, H. (1992) *Carbohydr. Res.*, **229**, 213–224.

Brade, H., Brabetz, W., Brade, L., Holst, O., Löbau, S., Lucakova, M., Mamat, U., Rozalski, A., Zych, K. and Kosma, P. (1997) *J. Endotoxin Res.*, **4**, 67–84.

Emsley, L. and Bodenhausen, G. (1992) *J. Magn. Reson.*, **97**, 135–148.

Fu, Y., Baumann, M., Kosma, P., Brade, L. and Brade, H. (1992) *Infect. Immun.*, **60**, 1314–1321.

Hwang, T.-L. and Shaka, A.J. (1992) *J. Am. Chem. Soc.*, **114**, 3157–3159.

Kosma, P., Bahnmüller, R., Schulz, G. and Brade, H. (1990) *Carbohydr. Res.*, **208**, 37–50.

Lian, L. Y., Barsukov, I. L., Sutcliffe, M. J., Sze, K. H. and Roberts, G. C. K. (1994) *Methods Enzymol.*, **239**, 657–700.

Massefski, W. and Redfield, A.G. (1988) *J. Magn. Reson.*, **78**, 150–155.

Mikol, V., Kosma, P. and Brade, H. (1994) *Carbohydr. Res.*, **263**, 35–42.

Moseley, H.N.B., Lee, W., Arrowsmith, C.H. and Krishna, N.R. (1997) *Biochemistry*, **36**, 5239–5299.

Ni, F. (1994) *Prog. NMR Spectrosc.*, **26**, 517–606.

Peters, T., Meyer, B., Stuike-Prill, R., Somorjai, R. and Brisson, J.-R. (1993) *Carbohydr. Res.*, **238**, 49–73.

Peters, T. and Pinto, B.M. (1996) *Curr. Opin. Struct. Biol.*, **6**, 710–720.

Scheffler, K., Ernst, B., Katopodis, A., Magnani, J. L., Wang, W.T., Weisemann, R. and Peters, T. (1995) *Angew. Chem., Int. Ed. Engl.*, **34**, 1841–1844.

Scherf, T. and Anglister, J. (1993) *Biophys. J.*, **64**, 754–761.
Stuike-Prill, R. and Meyer, B. (1991) *Eur. J. Biochem.*, **194**, 903–919.
Vincent, S.J.F., Zwahlen, C., Post, C.B., Burgner, J.W. and Bodenhausen, G. (1997) *Proc. Natl. Acad. Sci. USA*, **94**, 4383–4388.
Weimar, T., Harris, S. L., Pitner, J. B., Bock, K. and Pinto, B. M. (1995) *Biochemistry*, **34**, 13672–13680.
Weimar, T., Imberty, A., Perez, S. and Peters, T. (1997) *Theochem.*, **395**/**396**, 297–311.
Zwahlen, C., Vincent, S.J.F., Di Bari, L., Levitt, M.H. and Bodenhausen, G. (1994) *J. Am. Chem. Soc.*, **116**, 362–368.